Inverse methodology as applied to reconstruct local textile features from measured pressure field

S. Bancora, C. Binetruy, S. Advani, Sebastien Comas-Cardona

Version of Record: https://www.sciencedirect.com/science/article/pii/S1005030220307878
Manuscript_a336878d78b17cbd40618cc96813e968

Research Article

Inverse methodology as applied to reconstruct local textile features from measured pressure field

S. Bancora[a,*], C. Binetruy[a], S. Advani[b,a], S. Comas-Cardona[a]

[a] *École Centrale de Nantes, Research Institute in Civil Engineering and Mechanics (GeM), UMR CNRS 6183, 44321 Nantes Cedex 3, France*

[b] *Department of Mechanical Engineering, University of Delaware, Newark, Delaware 19716, USA*

[Received 1 April 2020; Received in revised form 29 May 2020; Accepted 14 July 2020]

Corresponding author
E-mail address: simone.bancora@ec-nantes.fr (S. Bancora)

Abstract

One can compute the final deformation of a known geometry under specific boundary conditions using the constitutive laws of mechanics that describe their stress strain behavior. In such cases the initial geometry is known, and all operators mapping the deformation are defined on the reference domain. However, there are situations in which the final configuration of a deformation might be known but not the initial. The inverse formulation allows one to determine the initial geometry of a domain, given its final deformation state, the material behavior law and a set of boundary conditions. In the present work we propose a method to reconstruct the mesoscale geometry of a textile based on its mechanical response during compaction. To do so, stress boundary conditions are acquired by means of a pressure-sensitive film. By adopting an appropriate material law, the thickness and width information of the yarns are deduced from the pressure field experienced by the compacted textile. Unlike 3D scanning techniques such as μ-CT, the proposed method can be applied on any domain size, allowing long-range variability to be captured. To the best of the authors' knowledge, there are no previous works that use a pressure-sensitive film on a large domain to capture the

input data for a shape reconstruction. This example application serves as a demonstration of a methodology which could be applied to other classes of materials.

Keywords

Textiles, Pressure sensors, Inverse method, Digital twin, Geometry reconstruction, Hyperelasticity

1. Introduction

Inverse formulations in mechanics allow to compute unknown properties of the study domain starting from available response or external boundary conditions. Many kinds of such methods exist: perhaps the most common example in mechanics is the identification of material parameters [1,2] or boundary conditions [3].

One possible application of inverse formulation is the detection of the unknown initial shape of a domain, when some information is available such as its deformed configuration or the boundary conditions applied. An extensive work on such application was presented in [4], where a full inverse finite element method was deployed to determine the initial shape of a rubber domain given some final conditions. Another example [5] is the reconstruction of the initial shape of an aortic aneurysm from the final configuration and the pressure experienced by the tissue. One big challenge in inverse methods is that they often rely on knowing some field variables of the final configuration: for example, in a mechanical deformation problem one might need to know the Cauchy stress experienced by the deformed domain, or the displacement field on some boundaries. An extensive theoretical treatment of the inverse application of boundary values can be found in [6]. The actual values however are not always easy to obtain due to physical shortcomings such as difficult sensors placement or limited measurable domain.

In this work we propose an inverse methodology for initial shape identification of a deformed domain from the knowledge of the final geometry and boundary pressure. The method is applied to the reconstruction of a glass-fiber textile composed of many yarns, which is subject to a planar compaction state between two parallel rigid plates. The final thickness of the domain is known, while the initial geometry (thickness, width and path) of each yarn are unknown and subject to individual variability from one yarn to another.

This material was chosen for several reasons. First, textiles are engineering materials widely used in composites manufacturing with applications in biomedical, automotive and aerospace. Second, textiles are a fitting example of materials which are compressed in a

mould where the final thickness is known but the initial one is not, nor is the real pressure field experienced by the material. Furthermore, textiles present a periodic architecture which is subject to intrinsic local variability at the scale of the single yarns [7,8]. Being able to identify these variations in geometry can be of great benefit to process control and digital characterization of properties such as hydraulic permeability [9]. Lastly, yarn deformation obeys the general framework of compressible hyperelasticity [10,11], therefore such behaviour could be adopted for many other classes of materials.

The measurement of the boundary pressure is achieved using a flexible pressure sensor. Technical developments of recent years spawned many examples of similar sensors based on current-resistive cells [12]. These sensors are typically very limited in both size and resolution due to added manufacturing costs and applications range from biological measurements [13,14] to process monitoring [15]. In this work the purely mechanical Prescale® sensor by Fujifilm is used. This is a pressure-sensitive film capable of registering a distributed pressure applied normally on its surface, yielding a quantification of the field in the form of a color intensity map. Since the measurement is carried out by the rupture of color-releasing microcapsules, this system is cheaper than the aforementioned electrical sensors. The Prescale® sensor has been extensively used in biomechanics to study contact surfaces, in articular joints [16,17] or other mechanical applications [18,19]. Other fields of application include studies on wheel/road [20] or wheel/rail [21] contact. This particular sensor works well with the chosen material, as it can be laid under the textile when a mould is closed during the compaction stage.

In addition to the mentioned cost effectiveness, another interesting advantage of this film is that the measurement has no limitations in size, unlike electrical sensors or direct geometry measurement techniques such as μ-CT which yield extremely accurate results but limited to a small material sample [22].

To the best of the authors' knowledge this is the first time a pressure-sensitive film is used as an input in an inverse identification method. The boundary pressure information and the final imposed thickness are used to compute the initial dimensions (thickness, width) of each individual yarn in the textile. As these dimensions are in the order of millimiters, an additional interest of this study is to assess if the measurement resolution of the Prescale® pressure film is still reliable at this scale.

Ultimately this work aims at providing a detailed methodology of inverse geometry reconstruction based on real pressure measurement, which could be extended to any other class of materials subject to a similar compression deformation.

2. Materials

The example textile we selected to be reconstructed is the UDT400 glass fabric ($A_w = 423\,\mathrm{g/m^2}$) from Chomarat. This unbalanced quasi-unidirectional woven fabric was chosen because the complexity of the structure is reduced due to the absence of noticeable yarn waviness, so that bending effects can be neglected. The fabric material is shown in Fig. 1.

3. Methodology

To reconstruct the initial geometry of the textile, an inverse formulation methodology of reconstruction is applied to every yarn. The method will be illustrated for one generic yarn, and later will be extended to the entire textile. The following assumptions are made:

- the length of the yarn is assumed to be much larger than the cross-sectional dimensions, therefore a 2D plane strain formulation can be justified. The yarn is oriented with its major axis (width) and minor axis (thickness) as illustrated in Fig. 2.
- the yarn cross section geometry of a yarn is described as a power ellipse as detailed in [23], with a measured shape parameter $n = 0.3$. Therefore identifying the cross-section geometry reduces to finding the value of thickness (h) and width (w) dimensions.
- The geometry is symmetric with respect to planes passing through the center O with normals $\boldsymbol{e}_1$ and $\boldsymbol{e}_2$.
- The yarn is modeled as a continuum.

Based on this premise, the stress state on the domain is only known at the boundaries, where the magnitude of the normal distributed traction vector $\Gamma\boldsymbol{e}_2$ can be measured (on the deformed domain) by the pressure sensor. By Cauchy's theorem the admissible stress state will imply:

$$\boldsymbol{e}_2\,\boldsymbol{\sigma}(\boldsymbol{x})\,\boldsymbol{e}_2 = \Gamma_{\mathrm{meas}} \quad \forall \boldsymbol{x} \in \partial\Omega_{\mathrm{film}} \tag{1}$$

where $\boldsymbol{x}$ is the position vector of a point in the deformed configuration, Γ_{meas} is the boundary pressure measured by the sensor and $\partial\Omega_{\mathrm{mould}}$ is the boundary subregion in contact with the mould. By describing the deformation behavior by an appropriate constitutive law the stress

state can be related to the deformation state. The inverse formulation then reduces to finding the deformation gradient $\boldsymbol{F}(\boldsymbol{x})$ that satisfies Eq. (1) for the known final configuration.

The methodology will be detailed in several steps.

- A suitable constitutive law will be chosen to relate the deformation of the yarn to the stress state (section 3.1)
- The identification of the material parameter of the constitutive law will be undertaken (section 3.2)
- The inverse problem will be formulated and validated on the reconstruction of a single yarn cross-sectional geometry (sections 3.3, 3.4)
- An example of large scale reconstruction will be given, by applying the method on a full textile (section 4)

3.1. Yarn constitutive law

Previous efforts have described the mechanical behavior of yarns under compaction. The reported modeling approaches can be broadly classified into micro-mechanical or continuum descriptions of the yarn. In our study, continuum approach to describe the yarn mechanical behavior is adopted.

This choice is justified by the fact that, although composed of many filaments or fibers, a yarn often behaves as a continuum body due to the closely packed small diameter filaments that form the yarn bundle and the presence of sizing which maintains its cohesion. However, it will be highly non-linear mechanical behavior, since a yarn deformation under a load is a motion of the fibers within. Dixit [24] modeled the yarn as an elastic material, transversely isotropic in directions normal to the yarn orientation and described the evolution of the elastic modulus as a function of fiber volume fraction. Recently Dharmalingam [10], Lectez [11] and Hemmer [25] studied the evolution of yarn cross sections under compaction and described the material behavior with a compressible hyperelastic constitutive law. They used a variation on the Ogden [26] strain energy density function known as hyperfoam material, that was proposed in 2000 by Jemiolo and Turtletaub [27]. This model is adopted in the present work.

The strain energy density function of the hyperfoam material is defined in terms of principal stretches λ_i as:

$$W(\lambda_1,\lambda_2,\lambda_3)=\frac{2\mu}{\alpha^2}\left(\lambda_1^{\alpha}+\lambda_2^{\alpha}+\lambda_3^{\alpha}-3+\frac{1}{\beta}\left(J^{-\alpha\beta}-1\right)\right) \tag{2}$$

where the principal stretches $\lambda_i=|\mathrm{d}\boldsymbol{x}|/|\mathrm{d}\boldsymbol{X}|$ are the eigenvalues of $\boldsymbol{F}$, $\boldsymbol{X}$ is the position vector of a point in the initial configuration, $J(\boldsymbol{F})$ is the determinant of the deformation gradient and α,β,μ are parameters that need to be identified. The orthonormal basis is placed so that $\boldsymbol{e}_3$ is aligned along the direction of the fibers and $\boldsymbol{e}_2$ is oriented in the thickness direction out of plane. Furthermore, inextensibility of the material in the fibers direction is assumed by setting $\lambda_3=1$. According to classical hyperelastic material theory, the eigenvalues of the Cauchy stress tensor are derived from Eq.(2) as:

$$\sigma_i=\frac{\lambda_i}{J}\frac{\partial W}{\partial\lambda_i} \tag{3}$$

where Voigt notation was adopted for the stresses:

$$\boldsymbol{\sigma}=[\sigma_{11},\sigma_{22},\sigma_{33},\sigma_{23},\sigma_{13},\sigma_{12}] \tag{4}$$

As stated in the assumptions, we simplify the problem according to plane strain theory. The principal Cauchy stresses in the cross-sectional plane are:

$$\sigma_1=\frac{2\mu}{\alpha\lambda_2}\left(\lambda_1^{\alpha-1}-\lambda_2^{-\alpha\beta}\lambda_1^{-\alpha\beta-1}\right) \tag{5}$$

$$\sigma_2=\frac{2\mu}{\alpha\lambda_1}\left(\lambda_2^{\alpha-1}-\lambda_1^{-\alpha\beta}\lambda_2^{-\alpha\beta-1}\right) \tag{6}$$

The yarn is free to laterally expand under compression in the $\boldsymbol{e}_2$, direction so we adopt the assumption that $\sigma_1=0$ at all locations of the domain. This yields from Eq. (5) a relation between principal stretches:

$$\lambda_1=\lambda_2^{-\frac{\beta}{1+\beta}} \tag{7}$$

and Eq.(6) can be simplified to:

$$\sigma_2 = \frac{2\mu}{\alpha}\left(\lambda_2^{\frac{\alpha+\alpha\beta+1}{1+\beta}} - \lambda_2^{\frac{-\alpha\beta-1}{1+\beta}}\right) \tag{8}$$

The coefficients α, β, μ need to be characterized for this specific material in order to exercise the model.

3.2. Material parameters identification

A set of compression tests were performed in order to identify the parameters of the model. The experimental apparatus used is shown in Fig. 3. It consists of an Instron 5584 machine, on which a ball joint was mounted to ensure parallelism between the top and bottom plates. A small punch-die compression assembly was used to better control the placement of the yarn. For each test, a single yarn of 5 cm of length was placed between the plates of the device and compacted at very low deformation velocity of 0.5mm/min. Values of force, displacement and time were recorded from the machine. The cross-section transformation during the compaction was recorded by a camera placed in front of the apparatus as shown in Fig. 4.

Measurements were taken from 8 compression repetitions. The evolution of width w and thickness h was extracted by image analysis from the bounding box of the cross sections, using the software ImageJ [28]. Consequently, the values of stretch in the principal directions are obtained as $\lambda_1 = h/h_0, \lambda_2 = w/w_0$ where h_0 and w_0 are respectively the thickness and width of the initial configuration (stress free). The β parameter is calculated first by fitting Eq. (7) to the recorded experimental measurements of λ_1, λ_2 and used to determine the yarn width according to the vertical compression λ_2 to obtain a Cauchy stress curve from the measured force. An assumption of homogeneous stress state is made. It is reasonable as the geometry of the yarn is almost rectangular. Although this simplification could lead to some inaccuracy in the material characterization, relaxing this assumption would require knowing the complete strain field in the cross section, which is not practical to achieve. The raw data collected is processed and the machine compliance is eliminated to yield a stress-deformation curve for 8 yarns tested. Measurements between all samples followed a coherent trend, with some differences due to the intrinsic variability that characterizes fiber yarns [22]. From this experimental data the material parameters α, μ are calibrated by mean square error

minimization. Experimental and fitted curves are plotted in Fig. 5. The values found for the model coefficients are: $\alpha = 44.8178, \beta = 0.1857, \mu = 0.8341$ MPa.

3.3. Inverse formulation

The objective of the problem is to determine the initial yarn cross section geometry in terms of width (w_0) and thickness (h_0) of a yarn under compression, given a final thickness h and a measured boundary pressure Γ_{meas}. The final thickness h is an arbitrary imposed value ($h < h_0$) and corresponds to the final gap between the compression plates. In the case of composite materials, it is a design parameter determined to obtain the desired fiber volume fraction [29]. Adopting the hyperfoam material law allows one to use Eq. (1) to formulate the problem stated below in Eq. (9):

$$\lambda_i = \arg\min_{\lambda_i} |\boldsymbol{e}_2\, \boldsymbol{\sigma}(\boldsymbol{x}, \lambda_i)\, e_2 - \Gamma_{meas}| \quad \forall \boldsymbol{x} \in \partial\Omega_{mould} \tag{9}$$

One simple formulation would be to use Eq. (9) to determine λ_2 for a given boundary pressure Γ_{meas} that could be measured by the mentioned pressure sensitive film whose color density evolves with pressure. Being λ_i the eigenvalues of the deformation gradient $\boldsymbol{F}(\lambda_i)$, the reference configuration could be determined with the pull-back operation:

$$\boldsymbol{X} = \boldsymbol{F}^{-1}\boldsymbol{x} \tag{10}$$

which in the chosen basis and for our simple transformation yields:

$$h_0 = \lambda_2^{-1} h \tag{11}$$

$$w_0 = \lambda_1^{-1} w = \lambda_2^{\frac{\beta}{1+\beta}} w \tag{12}$$

This approach however would only work if the stress state was perfectly homogeneous and for a simple rectangular geometry. When a yarn is compressed instead the measured stress Γ_{meas} exhibits a gradient of intensity, with a maximum value on the centerline, as shown in Fig. (10c).

Furthermore, since the final width w is unknown, Eq. (12) is not applicable right away. For this reason we look for some further condition to link w_0 to known quantities. The cross section geometries of a population of 8 yarns in the initial state were measured using a confocal scanner (profilometer). As already stated in the assumptions, these cross sections fit into power ellipses [23]. Width (w_0) and thickness (h_0) for each sample were extracted as the bounding box dimensions, and the area A_0 of each cross section is computed numerically from the profile, as listed in Table (1). From this sample space the average area $\bar{A} = 1.08\text{mm}^2$ and the standard deviation $\sigma = 0.049\text{mm}^2$ ($\approx 5\%$) are calculated. The very low deviation allows us to assume that for this particular material the initial cross section area remains constant in the reference state even though the yarn initial dimensions are affected by variability. Adopting this assumption the width w_0 of a yarn in the reference state can be directly expressed as a function of a given thickness h_0:

$$w_0(h_0) = \arg\min_{w_0}\left(\left|A(h_0, w_0) - \overline{A}\right|\right) \tag{13}$$

Using this assumption of constant initial cross section area, a finite element solution of the stress field is adopted to extract the inhomogeneous left-hand side term of Eq. (9).

To obtain such a solution, the compaction of the yarn is simulated iteratively in ABAQUS using an explicit method. An initial yarn cross section geometry is generated numerically, with an initial guess for thickness h_0^* and width w_0^* that satisfies Eq. (13) for a fixed value of $\overline{A}$. The yarn is assigned the hyperfoam material law with the identified parameters α, β, μ in the plane strain framework. A rigid 1D element which represents the mould is used to impose the final thickness h on the domain. From the finite element solution, the σ_2 Cauchy stress is computed, which as expected is quite homogeneous along the e_2 direction and inhomogeneous in the e_1 direction, as shown in Fig. (7). From the computed stress field, the normal pressure $\Gamma_{\text{num}}(h_0^*)$ at the rigid element boundary $\partial\Omega_{\text{mould}}$ is extracted.

Finally, using the stress value Γ_{meas} acquired from the Prescale® pressure-sensitive film, the error is calculated as:

$$\xi = \left|\Gamma_{\text{num}}(h_0^*) - \Gamma_{\text{meas}}\right| \tag{14}$$

Details on pressure acquisition and calibration of the film are provided in the Appendix A.

The initial thickness h_0 of the yarn is found as:

$$h_0 = \arg\min_{h_0^*} \xi(h_0^*) \tag{15}$$

and initial width w_0 is determined using Eq. (13) under the assumption of constant initial cross-section area $\overline{A}$.

This optimization is performed iteratively by assigning an arbitrary initial value h_0^*, performing the analysis and saving the resulting $\Gamma_{\text{num}}(h_0^*)$ to a file before starting over with a new value of h_0^*. The steps of this numerical optimization are summarized in Fig. 6.

The interest of saving all values of $\Gamma_{\text{num}}(h_0^*)$ for all possible values of h_0^* is to create a database that can be readily used to quickly evaluate Eq. (14) for a given h when multiple yarns are being reconstructed, each with their local value of Γ_{meas}. An example of $\Gamma_{\text{num}}(h_0^*)$ database for different yarn reference dimensions and a given final h is shown in Fig. 8.

3.4. Cross-section validation

The validation of the initial geometry reconstruction is performed by comparison with experimental measurements. A set of yarns were compressed up to an imposed thickness h and the whole transformation was recorded from a camera placed in front of the cross section as in Fig. 9(left). A Prescale® film was also placed under the yarn, and the pressure profile Fig. 9 (right) was used to identify the yarn geometry following the procedure just described. The geometry calculated from the pressure information was compared with the real yarn geometry measured from the video information for error quantification.

The results and a quantification of error are reported in Table 2, where w_0 and h_0 are the reference dimensions. The superscripts "meas" and "calc" indicate the measured and calculated values respectively. The imposed final thickness is $h = 0.25\text{mm}$. The percentage relative errors in the calculated quantities with respect to the measured ones are reported in parentheses.

The results of this section show that:

- it is possible to reconstruct with accuracy a yarn geometry in its initial configuration from a compressive test and a pressure field sensor.
- the resolution of the Prescale® pressure sensitive film is high enough to work well even on the relatively small yarn dimensions.

4. Full textile reconstruction

The interest of this work is to detail and showcase how stress boundary conditions can be applied for inverse method reconstruction of more complex domains and geometries. To showcase the potential of the technique presented in Section 3 for a single yarn, the reconstruction will be extended to a full textile which contains several yarns.

4.1. Cross sections

To address this scenario, the method is simply repeated for each yarn, since by laying the entire textile sample over a layer of Prescale® film and compressing it is possible to know the pressure field Γ^i_{meas} experienced by every i^{th} yarn individually. A UDT400 textile was placed on the pressure film and compressed up to an imposed final thickness h. From the resulting pressure print an area of $98\ \text{mm} \times 98\ \text{mm}$, corresponding to a collection of 33 weft yarns and 27 warp yarns, was extracted to be analyzed. This frame can be seen in Fig. 11(b).

For each individual yarn, multiple intensity measures are sampled from the pressure print along its length and in between crossover points, as shown in Fig. 10(b). The measures are averaged length-wise to compute the curve of pressure Γ^i_{meas} relative to the i-th yarn as shown in Fig. 10(c). Assigning a length-averaged pressure profile and therefore a constant cross-section identification to each yarn simplifies the geometry identification process. Each pressure curve is used in Eq. (15) to find the corresponding yarn reference dimensions (h_0, w_0) under the assumption of known initial cross-section area $\overline{A} = 1.08\ \text{mm}^2$. It should be noted that this method can allow for the cross-section to vary along the yarn length by simply repeating the identification at every sampling instead of length-averaging the pressure print. However this was not taken into account as it would be material specific and the number of identifications to carry out increases especially on a large domain.

4.2. Yarn paths

When a full textile is being reconstructed it is not sufficient to determine the yarn cross section geometries, but yarn paths are needed as well as this is important for investigating dual scale flow when these textiles are impregnated with resin [30]. These could easily be measured by imaging techniques, taking a picture of the textile to have realistic yarn paths as was done by Gommer et al. [7]. However since the pressure field measured by the Prescale® film contains spatial information as well, the yarn paths can be directly extracted from that measurement. The complexity of this step depends on the complexity of the textile

architecture. In this study, since the textile is woven material, the regions where the weft and warp yarns cross over are clearly visible as spikes in pressure since the thickness is locally higher. The yarn paths are easily measured by interpolating a spline through these regions. At the current level of implementation, the yarn paths definition is performed manually by using the ImageJ software to select and output the nodal positions $C(x, y)$ of crossover regions on the domain as shown in Fig. 10(a). To these in-plane coordinates the z information is added by shifting the nodes out of plane following the weaving pattern to account for the thickness of the warp yarn, which was assumed to be non-deformable. These nodes $C(x, y, z)$ are used for the definition of each yarn path when the textile geometry is generated.

4.3. Geometry generation

Following the method proposed, the information of initial cross section and yarn path for each individual yarn has been obtained. In order to generate the 3D geometry, the textile geometry generator TexGen [31] is used through scripting.

The original textile, compaction pressure map and reconstructed geometry can be seen in Fig. 11. It is clearly visible that the yarn paths and geometries are not idealized, but exhibit instead the variability in cross-section and path that was captured from the pressure print.

5. Summary and conclusions

Through a specific application, an inverse methodology was detailed to identify the dimensional parameters of a domain and reconstruct its initial geometry. The procedure has been showcased on the reconstruction of a textile under compression, but the principle could be applied to other contexts. The method is based on the acquisition of boundary values of pressure experienced by the material in the process, which was achieved using a pressure sensitive film. The hyperfoam material model was used to relate the pressure to the deformation of the yarns, and therefore to the reference geometry.

A final example of reconstruction of an extended textile was provided, by using the pressure film to extract the yarn paths as well as the cross sectional geometries of each yarn. This large scale reconstruction showcases the potential of using Prescale® film, as there are no limitations in domain size with this sensor and methodology (unlike for example µ-CT or image processing). Answering one stated objective, validation carried out yarn-wise showed a good match between the reconstructed and measured geometry, proving that the sensitivity of the film is satisfactory even on very small scales.

Being able to reconstruct the detailed textile geometry opens up the possibility of performing further analysis on the domain, such as computing the expected hydraulic permeability or assessing quality control over variability. However it is important to state that the reconstruction of a single layer of textile has very little direct application, and the material was chosen for this study as representative for the motivations listed in the introduction. This approach could be extended to curved surfaces due to textile deformation [32,33] or any other class of materials which exhibit similarities in mechanical behaviour and deformation mode.

Acknowledgements

This research was partially funded by Conseil Regional Pays de la Loire (grant number TEU29). The authors wish to thank A. Hautefeuille and the team at ECN GeM laboratory for the help with the experimental setup.

References

[1] S. Avril, F. Pierron, Int. J. Solids Struct. 44 (2007) 4978– 5002.

[2] Z.S. Ma, Y. C. Zhou, S.G. Long, C.S. Lu, J. Mater. Sci. Technol. 28 (2012) 626–635.

[3] B.H. Dennis, G.S. Dulikravich, in: M. Tanaka, G.S. Dulikravich (Eds.), Inverse Problems in Engineering Mechanics, Elsevier Science Ltd, 1998, pp. 61-70.

[4] T. Yamada, in: S.N. Atluri, G. Yagawa, T.A. Cruse (Eds.), Computational Mechanics' 95, Springer, Berlin, Heidelberg, 1995, pp. 2456-2461.

[5] J. Lu, X. Zhou, M.L. Raghavan, J. Biomech. 40 (2007) 693–696.

[6] M. Bonnet, A. Constantinescu, Inverse Probl. 2 (2005) R1-R50.

[7] F. Gommer, L.P. Brown, R. Brooks, J. Compos. Mater. 50 (2016) 3255–3266.

[8] K.D. Potter, in: International Conference on Composite Materials (ICCM)-17, Edinburgh, UK, 2009, pp. 18–25.

[9] M. Bahrami, M.M. Yovanovich, J.R. Culham, J. Fluid Eng. 128 (2006) 1036–1044.

[10] A.S. Dharmalingam, J. Hemmer, A.S. Lectez, C. Binetruy, S. Comas-Cardona, Compos. Part B-Eng. 148 (2018) 235–242.

[11] A. S. Lectez, K. E. Azzouzi, C. Binetruy, S. Comas-Cardona, E. Verron, J.-M. Lebrun, J. Compos. Mater. 52 (2018) 2661–2677.

[12] W. Chen, X. Yan, J. Mater. Sci. Technol. 43 (2020) 175-188.

[13] S.C. Mannsfeld, B.C. Tee, R.M. Stoltenberg, C.V.H. Chen, S. Barman, B.V. Muir, A.N. Sokolov, C. Reese, Z. Bao, Nat. Mater. 9 (2010) 859–864.

[14] S. Lee, A. Reuveny, J. Reeder, S. Lee, H. Jin, Q. Liu, T. Yokota, T. Sekitani, T. Isoyama, Y. Abe, Nat. Nanotechnol. 11 (2016) 472.

[15] W.A. Walbran, S. Bickerton, P.A. Kelly, Compos. Pt. A-Appl. Sci. Manuf. 40 (2009) 1119–1133.

[16] P. MacDonald, A. Miniaci, P. Fowler, P. Marks, B. Finlay, Knee Surg. Sport. Tr. A. 3 (1996) 252–255.

[17] A.B. Liggins, in: J.C. Shelton, J.F. Orr (Eds.), Optical Measurement Methods in Biomechanics, Springer, Boston, MA, 1997, pp. 173-189.

[18] H. Aritomi, M. Morita, K. Yonemoto, J. Biomech. 16 (1983) 157–165.

[19] Y. Kitafusa, The Bulletin of Tokyo Dental College 45 (2004) 99–108.

[20] P.W. Backx, Tyre/road Contact Measurement Using Pressure Sensitive Films, Eindhoven University of Technology, 2007.

[21] F. Dörner, C.H. Körblein, C.H. Schindler, Wear 317 (2014) 241–245.

[22] F. Desplentere, S.V. Lomov, D.L. Woerdeman, I. Verpoest, M. Wevers, A. Bogdanovich, Compos. Sci. Technol. 65 (2005) 1920–1930.

[23] M. Sherburn, Geometric and Mechanical Modelling of Textiles, Ph.D. Thesis, University of Nottingham, 2007.

[24] A. Dixit, R.K. Misra, H.S. Mali, Procedia Mater. Sci. 6 (2014) 1143–1149.

[25] J. Hemmer, A.-S. Lectez, E. Verron, J.-M. Lebrun, C. Binetruy, S. Comas-Cardona, J. Compos. Mater. 54 (2020) 3261-3274.

[26] R.W. Ogden, Non-linear Elastic Deformations, Courier Corporation, 1997.

[27] S. Jemiolo, S. Turteltaub, J. Appl. Mech. 67 (2000) 248–254.

[28] C.A. Schneider, W.S. Rasband, K.W. Eliceiri, Nat. Methods 9 (2012) 671.

[29] S.G. Advani, E.M. Sozer, Process Modeling in Composites Manufacturing, 2ed., Taylor and Francis Group, Boca Raton, FL, 2010.

[30] J. Slade, K. Pillai, S. Advani, Polym. Compos. 22 (2001) 491–505.

[31] H. Lin, L.P. Brown, A.C. Long, Adv. Mater. Res. 331 (2011) 44–47.

[32] S. Bickerton, E. Sozer, M. Graham, Compos. Pt. A-Appl. Sci. Manuf. 31 (2001) 423–438.

[33] P. Šimácek, S. Advani, S. Bickerton, Compos. Pt. A-Appl. Sci. Manuf. 31 (2001) 439–458.

[34] A.B. Liggins, J.C.E. Stranart, J.B. Finlay, C.H. Rorabeck, E.G. Little, in: Proceedings of the International Conference on Experimental Mechanics, Limerick, Ireland, 4-5

September, 1992

[35] A.B. Liggins, J.B. Finlay, Exp. Tech. 21 (1997) 19–22.

Figure list:

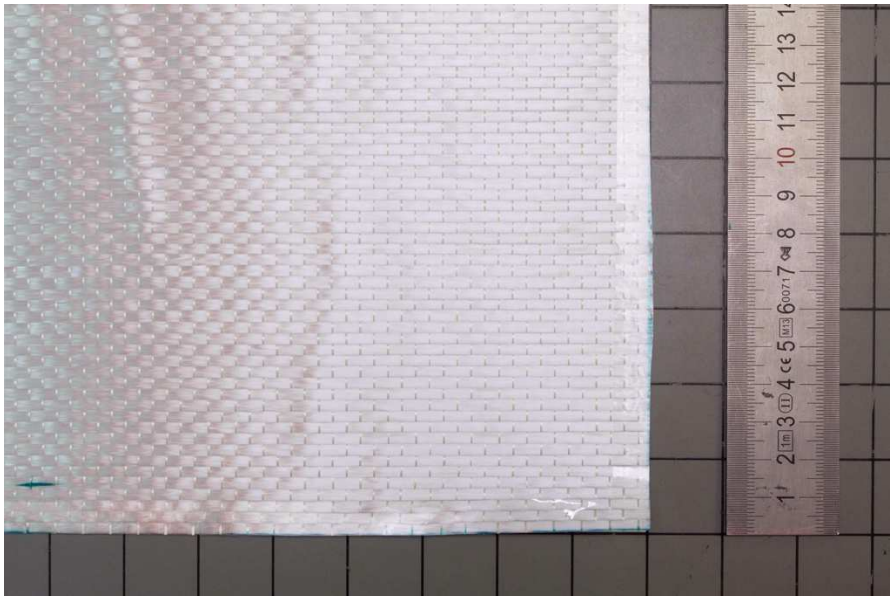

Fig. 1. UDT400 fabric.

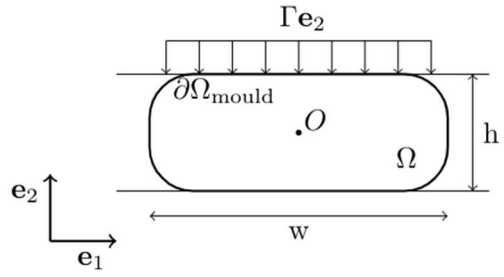

Fig. 2. Schematic of Yarn cross section where w is the width and h is the thickness subjected to normal distributed traction vector, $\Gamma \boldsymbol{e}_2$

Fig. 3. Single yarn compression device.

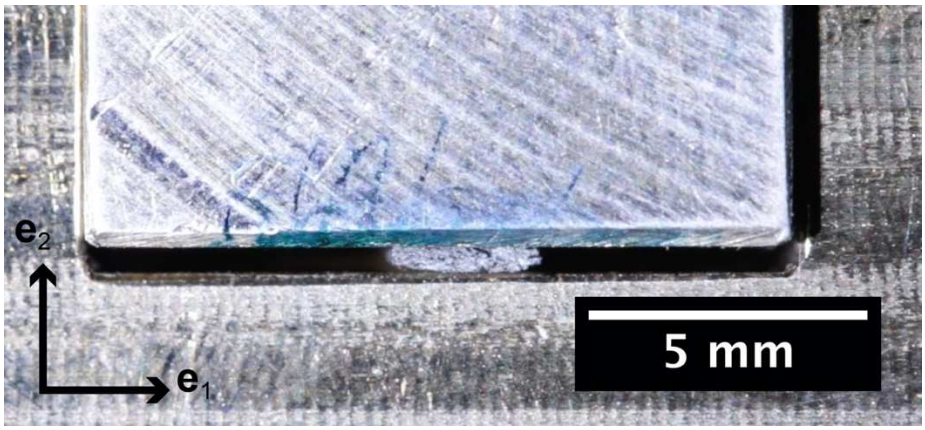

Fig. 4. Camera recorded yarn compression.

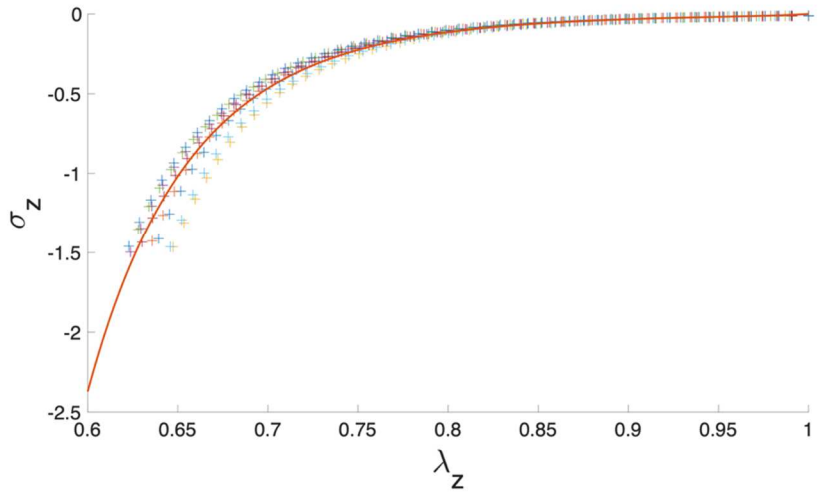

Fig. 5. Stress/stretch best curve fitting provided the model coefficients: $\alpha = 44.8178, \beta = 0.1857, \mu = 0.8341$ MPa in Eq. (2).

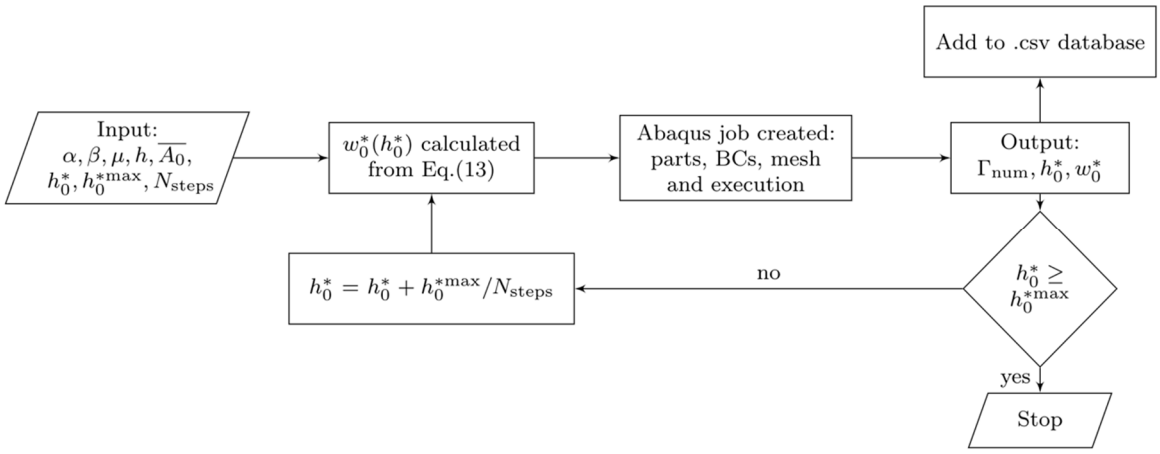

Fig. 6. Flowchart to create the stress/initial geometry database.

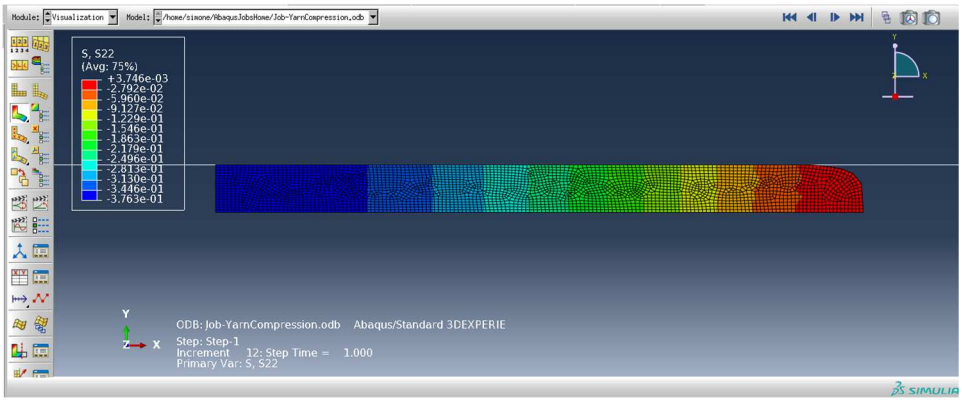

Fig. 7. Finite element yarn compression, σ_2 stress field on a quarter of yarn.

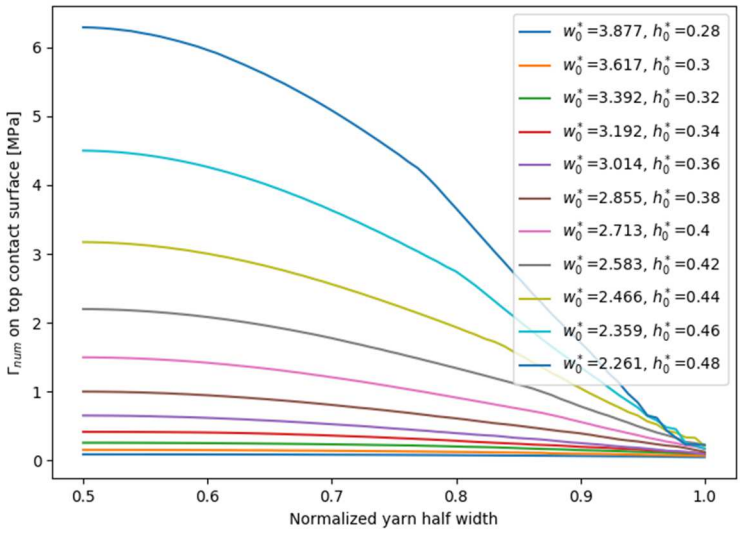

Fig. 8. Γ_{num} database for imposed final $h = 0.25$mm, half yarn normalized width (vertical symmetry). Units in legend are [mm].

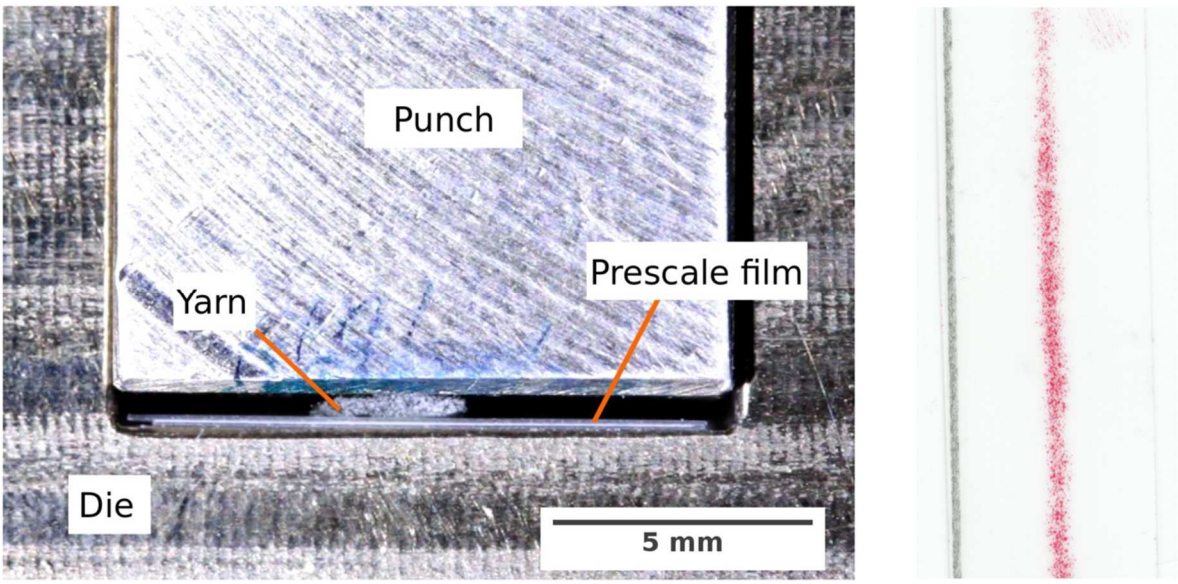

Fig. 9. Visual validation of yarn geometry reconstruction (left) and pressure print of one yarn (right).

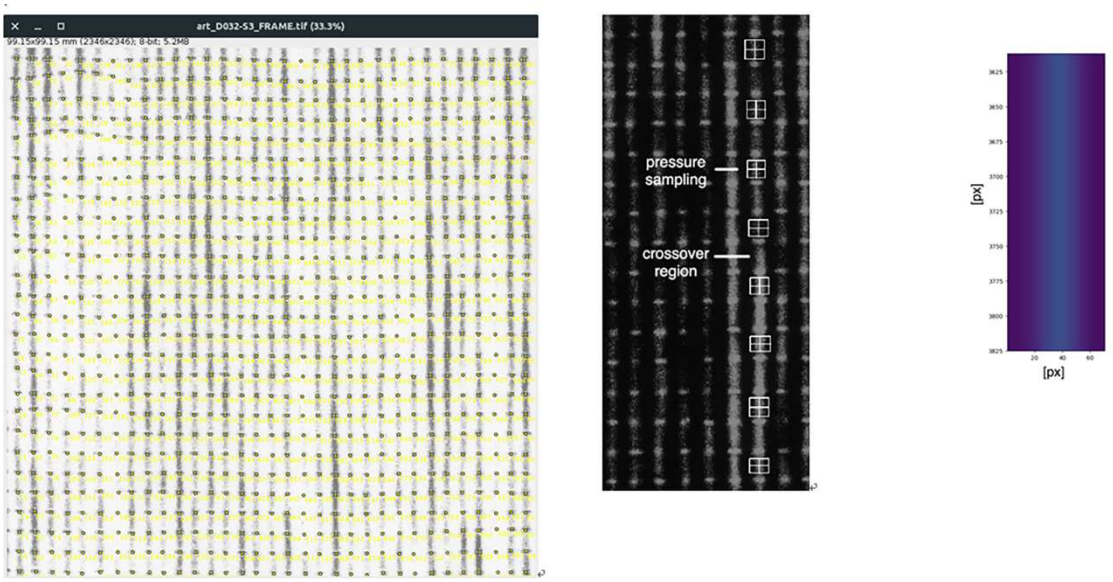

(a) Pressure field used for the UDT400 textile reconstruction. Nodes are marked at the crossover regions.

(b) Inter crossover sampling on yarn i

(c) Longitudinally averaged pressure profile Γ^{i}_{meas}

Fig. 10. Pressure field analysis for the textile reconstruction.

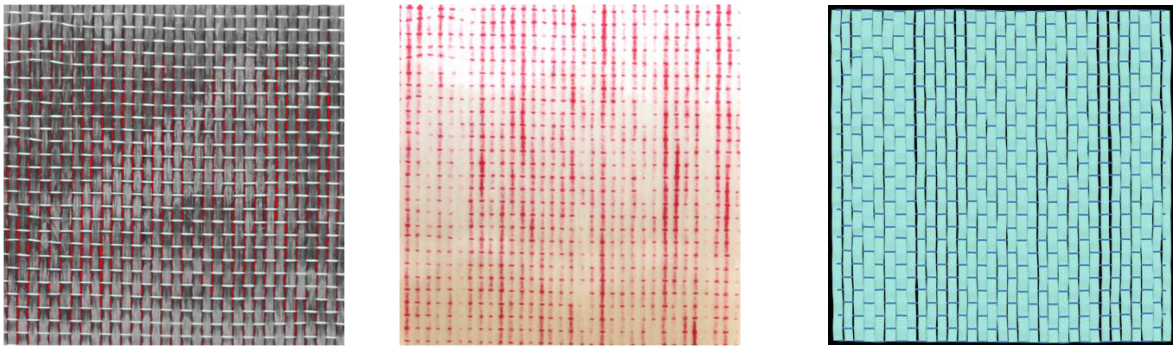

(a) Picture of the real material (intra-yarn gaps highlighted)

(b) Prescale pressure field

(c) Reconstructed material

Fig. 11. Synoptic comparison of real and reconstructed geometry of a 98 × 98mm UDT400 textile.

Table list:

Table 1 *Measured reference cross-section area A_0 from an 8 samples population.*

Yarn sample	1	2	3	4	5	6	7	8
A_0 [mm^2]	1.10	1.11	1.11	1.09	1.12	1.08	1.04	1.12

Table 2 Comparison of reconstructed vs measured yarn geometries [mm].

Specimen	w_0^{meas}	h_0^{meas}	w_0^{calc}(err)	h_0^{calc}(err)
1	2.94	0.35	3.192(8.5%)	0.34(2.8%)
2	3.39	0.33	3.392(0.05%)	0.32(3%)
3	2.7	0.41	2.65(1.8%)	0.405(1.2%)
4	2.7	0.41	2.77(2.6%)	0.4(4.8%)
5	3.42	0.34	3.39(1%)	0.32(5.8%)
6	2.75	0.39	2.855(3.8%)	0.38(2.6%)